

Hydrophobic Modification of Sulfonated Carbon Aerogels from Coir Fibers To Enhance Their Catalytic Performance for Esterification

Ade Sonya Suryandari, Tantular Nurtono, Widiyastuti Widiyastuti, and Heru Setyawan*

Cite This: *ACS Omega* 2023, 8, 27139–27145

Read Online

ACCESS |

Metrics & More

Article Recommendations

ABSTRACT: The hydrophilicity of sulfonic acid-functionalized solid catalysts tends to accelerate the deactivation of the catalyst for chemical reactions where water is produced during the process. In this work, we proposed a hydrophobic carbon aerogel acid catalyst derived from coir fibers by a sulfonation-hydrophobization route via the diazo reduction method. Sulfonation using the diazo reduction method offers some advantages such as the process takes only a few minutes and the modified surface can be easily modified further to be hydrophobic. The carbon aerogel was produced by direct pyrolysis of cellulose aerogels derived from coir fibers using an NH_4OH –urea method and then sulfonated and hydrophobized using sulfanilic acid and 4-*tert*-butylaniline (TBA), respectively. The carbon aerogel exhibited a very high surface area (2624.93 – $3911.05 \text{ m}^2 \text{ g}^{-1}$), which provides a lot of number of sites for sulfonate groups (2.30 – 2.70 mmol g^{-1}). The water contact angle of the sulfonated catalyst after hydrophobization ranged from 70 to 115° , depending on the mass ratio of the TBA-to-solid catalyst. The hydrophobic catalyst exhibited better catalytic performance toward esterification of acetic acid with ethanol. A conversion of 65 – 74% could be achieved in a brief time using the hydrophobic catalyst. The conversions were much higher than that obtained by the unmodified hydrophilic catalyst. Our study offers a strategy to tune the surface hydrophobicity of the sulfonated solid acid catalyst to match for specific chemical reactions.



1. INTRODUCTION

Biodiesel, one of the renewable fuels derived from biomass, is regarded as an environmentally friendly fuel due to its low emissions, high cetane number, flash point, and high combustion efficiency while being used directly or in a mixture with an average mixture ratio of 30 – 50% .^{1,2} Esterification of carboxylic acids with alcohols is one of the methods to produce biodiesel. Strong mineral acids like phosphoric acid (H_3PO_4), sulfuric acid (H_2SO_4), and hydrochloric acid (HCl) are typically used as homogeneous catalysts in esterification reactions to accelerate the reactions.^{1,3–6} However, homogeneous strong acid catalysts are toxic, corrosive, difficult to recycle, environmentally unfriendly, and less cost-effective due to the multiple stages of washing to purify the biodiesel product.^{2,7–9} The utilization of solid catalysts is considered to be able to overcome the drawbacks of homogeneous catalysts due to the ease of product separation and reusability that cause less environmental harm while reducing the production cost.^{3–5,10}

Sulfonated ordered mesoporous carbons (OMCs) have been extensively studied as solid acid catalysts and have shown good performance for esterification reactions. OMCs are typically prepared through a nanocasting method from carbon precursors (e.g., glucose, sucrose, and furfuryl alcohol) by

the pyrolysis process along with ordered mesoporous silica (OMS) templates (e.g., MCM-41 and SBA-15). The main steps to prepare the OMCs using this method are: (i) preparation of OMS, (ii) impregnation of carbon precursors into the OMS, (iii) pyrolysis, and (iv) removal of the OMS. The OMSs are typically prepared by the catalytic hydrolysis and condensation of silicon alkoxides using polymers or surfactants as templates. Hydrofluoric acid (HF), a very corrosive acid, is typically used to completely remove the OMS template, making the process harmful and environmentally unfriendly.^{11–13} We have proposed sulfonated carbon aerogels (SCAs) prepared by incomplete carbonization of cellulose aerogels derived from coir fibers as solid acid catalysts for esterification reactions.¹⁴ Although carbon aerogels are a nonordered material, they have a high specific surface area and pore volume and when sulfonated with sulfuric acid and they

Received: April 3, 2023

Accepted: July 12, 2023

Published: July 24, 2023



have good catalytic performance for esterification reactions. The inherent hydrophilic characteristics of solid acid catalysts produced using sulfuric acid as the sulfonation agent adversely influenced their catalytic performance due to the production of water as a byproduct in during the reaction.^{15–18} Because the esterification reaction is reversible, the reaction is hindered by water produced during the reaction, which tends to remain on the hydrophilic catalyst surface. To improve the catalytic performance of the solid acid catalyst for the esterification reaction, the catalyst surface must be modified in such a way that its properties are changed from hydrophilic to hydrophobic.¹⁹

This work reports on the preparation of hydrophobic solid acid catalysts based on carbon aerogels derived from coir fibers, an agricultural waste and abundant natural material with a cellulose content ranging from 23 to 43%, via the cellulose aerogel route.^{20,21} Previously, it has been mentioned that the hydrophilic properties of the catalyst surface might be caused by the inherent properties of H₂SO₄ as the sulfonating agent. Therefore, sulfanilic acid was used instead of H₂SO₄ as the sulfonating agent in the present work. The use of 4-*tert*-butylaniline (TBA) would enable hydrophobization on the surface of SCAs. The diazo reduction route was applied to graft aromatic groups on carbon substrates through the reduction reaction of sulfanilic acid and TBA as an aromatic amine reagent in the presence of sodium nitrite and hydrochloric acid. The highly porous carbon aerogel produced by the pyrolysis of cellulose aerogels was expected to enhance the grafting process of sulfonate groups to obtain solid acid catalysts with high density of active sites. Moreover, the controlled hydrophobicity of the catalyst surface was expected to eliminate the possibility of the byproduct in the form of water blocking the active side of the catalyst. The esterification reaction between acetic acid and ethanol was used to evaluate the performance of the catalyst.

2. EXPERIMENTAL SECTION

2.1. Preparation of the Carbon Aerogel. Following our proposed method,¹⁴ the carbon aerogel was prepared by pyrolyzing cellulose aerogels derived from coir fibers with the ammonia–urea cross-linking system. The coir fiber was ground, sieved at a size of 120 mesh, and digested in a solution of 6% sodium hydroxide (NaOH; Merck; reagent grade), at a ratio of 1 g of coir fiber/20 mL of alkali solution under atmospheric reflux for 4 h. Typically, 1 g of pulp (dry basis) was dissolved into solution containing 4 g of urea (CH₄N₂O; PT. Petrokimia Gresik, Indonesia), 11 mL of ammonia 25% (NH₄OH; Merck; reagent grade), and 5 mL of demineralized water, which was then stirred for 15 min and ultrasonically processed for 30 min. Prior to thawing naturally to room temperature, the gel formation was maintained at –5 °C for 24 h. Additionally, the gel was immersed in 15 mL of 98% ethanol (C₂H₅OH; Merck; reagent grade) and permitted to coagulate for 24 h. The gel was placed in a freezer at –20 °C for 24 h after being soaked in demineralized water to exchange ethanol with water. Freeze-drying was carried out for 24 h at a temperature of –45 °C under vacuum pressure (20 Pa). Because our previous work reported that the degradation of cellulose to carbon in aerogels cellulose–NH₄OH initiated at a temperature range of 330–490 °C,²² the current study was extended by varying the pyrolysis temperature to 500–700 °C. The cellulose aerogel was then pyrolyzed in a tubular furnace (Thermo Scientific TF55030C-1, tube ID = 18.1 mm, L = 50

cm, heating zone = 30.5 cm) under an inert atmosphere with a N₂ flow rate of 100 mL/min. Initially, the impurities in gas were eliminated from the sample by injecting 150 mL/min N₂ gas into it for 15 min. To eliminate moisture content, the temperature of pyrolysis was maintained at 150 °C for 30 min and increased to 400 °C for 30 min to decompose cellulose and evaporate volatile substances. The temperature was increased to 500–700 °C and kept for 2 h to allow the carbonization process.

2.2. Preparation of the Catalyst. The carbon aerogel was sulfonated using the diazo reduction method.²³ Typically, a mixture of 1 g of carbon aerogel and 0.1 M sulfanilic acid solution (H₃NC₆H₄SO₃; Merck; reagent grade) (1:1 mass ratio of carbon aerogel to sulfanilic acid) was heated at 70 °C under vigorous stirring conditions. An equimolar amount of sodium nitrite (NaNO₂; Merck; reagent grade) and sulfanilic acid was added to the mixture after the sulfanilic acid had been neutralized with 0.1 M NaOH solution. Additionally, 4.3 mL of 4 M hydrochloric acid solution (HCl 37%; Mallinckrodt; reagent grade) was added dropwise, and the grafting reaction was carried out for 10 min. The obtained sulfonated carbon aerogel named SCA was washed with demineralized water until the pH of the filtrate reached a neutral condition and dried at 80 °C for 12 h. The hydrophobization of the acidic carbon aerogel was carried out following the same method utilizing TBA ((CH₃)₃CC₆H₄NH₂; Merck; reagent grade), 1 g of SCA, and 0.48 g of NaOH dispersed in the mixture of ethanol (40 mL) and demineralized water (80 mL) and heated at 70 °C by stirring. Furthermore, NaNO₂ with an equimolar amount to TBA was introduced into the mixture. After 8 mL of 4 M HCl had been slowly dropped, the grafting process was completed in 10 min. The solid catalyst was washed until the pH of the filtrate reached a neutral condition and dried at 80 °C overnight. The obtained hydrophobic SCA was given the name HSCAx, where *x* represents the mass ratio of TBA to SCA.

2.3. Characterization. The morphology of the carbon aerogel was examined by scanning electron microscopy (SEM; FlexSEM 100, Hitachi). The identification of functional groups of the catalyst was detected using Fourier transform infrared spectroscopy (FTIR; IRTracer-100, Shimadzu) with a scanning range of 400–4000 cm^{–1}. The specific surface area of samples was measured using a N₂ adsorption–desorption instrument (NOVA 1200, Quantachrome). First, the sample was degassed at 300 °C for 3 h before N₂ adsorption at –196 °C. The specific surface area was determined using the Brunauer–Emmett–Teller (BET) plot of the nitrogen adsorption isotherm. Acid density was estimated using the neutralization titration method.²⁴ In typical, 0.05 g of the sample was immersed in 30 mL of 0.02 M NaOH, followed by an ultrasonic process (40 kHz) for 1 h. The solid sample was removed, and the filtrate was titrated with 0.01 M HCl in the presence of phenolphthalein. The concentration of the remaining OH[–] ions was determined by assuming that the amount of supplied H⁺ ions from HCl was equivalent to the amount of consumed OH[–] ions. Therefore, the acid density was calculated as the amount of OH[–] consumed (mmol) divided by the weight of the sample (g). The contact angle of the water droplet dropped on the catalyst surface was used to characterize the hydrophobicity properties of the catalyst. The photograph of the water droplet was taken by a digital camera with a macro lens and the contact angle was measured. The bulk density of aerogels ρ_b was calculated by dividing the

measured mass (m) by the measured volume (V) of the aerogel. Then, the porosity of the aerogel was calculated as

$$\phi = \left(1 - \frac{\rho_b}{\rho_t} \right) \quad (1)$$

where ρ_t is the true density of cellulose (1.528 g cm^{-3}).²⁵

2.4. Catalytic Reactions. According to our previous work,¹⁴ the catalytic performance of the solid acid catalysts was evaluated for esterification of acetic acid with ethanol. The esterification was performed in a three-neck flask equipped with a reflux condenser and heated by a heating mantle with a temperature controller and a magnetic stirrer. The molar ratio of acetic acid and ethanol was fixed at 1:2 with a catalyst loading of 0.01 g/g acetic acid. The reaction was carried out at 80 °C under stirring for 3 h. The progress of the reaction was followed by periodically sampling from the reaction mixture and the conversion was determined by analyzing the acetic acid concentration using gas chromatography (GC; Thermo Scientific, TRACE 1310). The gas chromatograph was equipped with a flame ionization detector (FID) and a Thermo Scientific column of type TG-SMS (30 m; 0.25 mm; 0.25 mm). The input injector, which was set up at 125 °C with a split ratio of 1:150 and nitrogen carrier gas flowing at 1 mL/min, was then used to inject 0.5 μL of each sample. The analysis was started at a temperature of 45 °C and it was maintained at this temperature for 3 min before being heated to 125 °C at a rate of 60 °C/min. Next, the temperature was cooled to 45 °C. Isobutanol was added as an internal calibration to determine the unreacted acetic acid. The esterification conversion of acetic acid was calculated as

$$\text{conversion of acetic acid (\%)} = \frac{n_i - n_f}{n_i} \times 100\% \quad (2)$$

where n_i and n_f are the initial and final mole numbers of acetic acid in the reaction mixture, respectively.

3. RESULTS AND DISCUSSION

3.1. Characteristics of the Carbon Aerogel. The cellulose aerogel derived from coir fibers using ammonia-urea cross-linking solution followed by freeze-drying was cylindrical in shape, with an average diameter and height of 4.04 and 0.72 cm, respectively (insets of Figure 1). The cellulose aerogel was light brown in color and very light due to its very high porosity. As shown in Figure 1, a leaf with the cellulose aerogel put on it was not deflected down due to its lightweight with an average mass of 0.9 g. The porosity, density, and specific surface area of the cellulose aerogel were 93.46%, 0.1 g cm^{-3} , and $557.18 \text{ m}^2 \text{ g}^{-1}$, which meets the range values of typical aerogel materials (porosity 90–99%, density $0.001\text{--}1 \text{ g/cm}^3$, and $100\text{--}1600 \text{ m}^2 \text{ g}^{-1}$).^{26,27}

To produce carbon aerogels, the cellulose aerogel was directly pyrolyzed under a nitrogen atmosphere at various temperatures to determine its effect on its characteristics. Figure 2 shows SEM images of the carbon aerogels produced at various pyrolysis temperatures. After pyrolysis, the color of the aerogels changed to black (insets of Figure 2), showing that cellulose had been degraded to carbon. The carbon aerogel produced had porous structures and comprised a three-dimensional network of interconnected fibers having a cylindrical shape, which inherited the microstructure of the original cellulose aerogel. The size of the carbon aerogel fibers, compared to that of the initial cellulose aerogel fibers, became

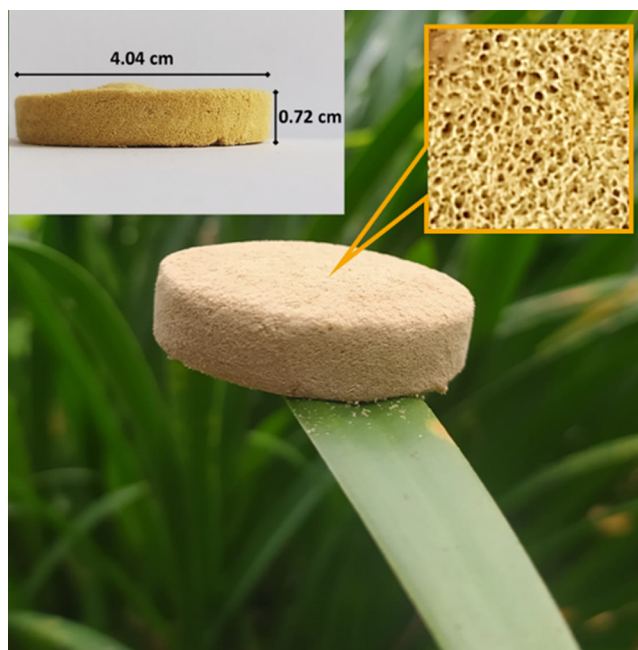


Figure 1. Physical appearance of the cellulose aerogel. The inset shows the size of the cellulose aerogel.

smaller as the pyrolysis temperature increased. The morphology of carbon aerogel fibers produced at a pyrolysis temperature of 500 °C is cylindrical fibers with intact structures and lines on their surface. Observing the cross-section of the carbon aerogel fibers, they had many pores with an irregular shape and arrangement. When the pyrolysis temperature was increased, the size of fibers became smaller and the pores inside the fibers collapsed, leaving the fiber with a broken wall structure. The shrinkage of fibers and the collapse of their internal pores were more severe when the pyrolysis temperature was increased further.

Table 1 shows the characteristics of carbon aerogels pyrolyzed at various temperatures. The pyrolysis yield, defined as the mass ratio of the carbon aerogel produced to the cellulose aerogel, tended to decrease from 22.71 to 17.68% with the increase of pyrolysis temperature at 500–700 °C. During pyrolysis, volatile matters in the cellulose aerogel were cracked and their phases changed into liquid and gas with lower molecular weights, hydroxyl groups were dehydrated, and cellulose and lignin were decomposed.^{28–30} At a pyrolysis temperature of 500–700 °C, the average pore diameter and the average fiber diameter were decreased from 4.71 to 3.82 and 58.52 to 34.80 μm , respectively. Although the pore size inside the fibers decreased, the BET surface area of the carbon aerogel significantly increased from 2624.93 to 3911.05 $\text{m}^2 \text{ g}^{-1}$ with an increase in pyrolysis temperature. This may be caused by the formation of more internal pores with smaller pore size left by the evaporated volatile matters during pyrolysis at higher temperatures.^{30,31}

Figure 3 shows the FTIR spectra of the cellulose aerogel and the corresponding carbon aerogels obtained by pyrolysis at various temperatures. The FTIR spectra of the cellulose aerogel shows a peak at a wavenumber of 3339 cm^{-1} , which corresponds to the O–H functional group derived from the hydroxyl group on cellulose.^{25,32} The peaks around 3270 and 1595 cm^{-1} are associated with the N–H group of urea. Moreover, the bands at 1661 and 1051 cm^{-1} were attributed to

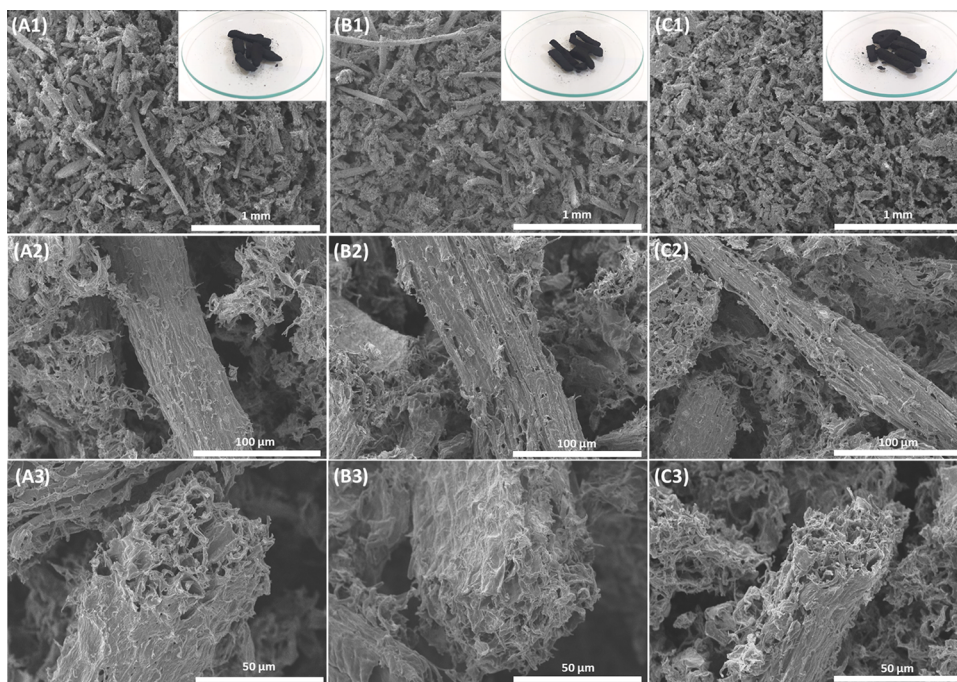


Figure 2. SEM images of the carbon aerogel obtained in various pyrolysis temperatures: (A1–A3) 500 °C, (B1–B3) 600 °C, and (C1–C3) 700 °C. The inset pictures show the photograph of the carbon aerogel.

Table 1. Characteristics of Carbon Aerogels Pyrolyzed at Various Temperatures

temperature (°C)	yield (%)	average pore diameter (μm)	average fiber diameter (μm)	surface area (m ² g ⁻¹)
500	22.71	4.71	58.52	2624.93
600	19.44	4.21	53.73	3118.42
700	17.68	3.82	34.80	3911.05

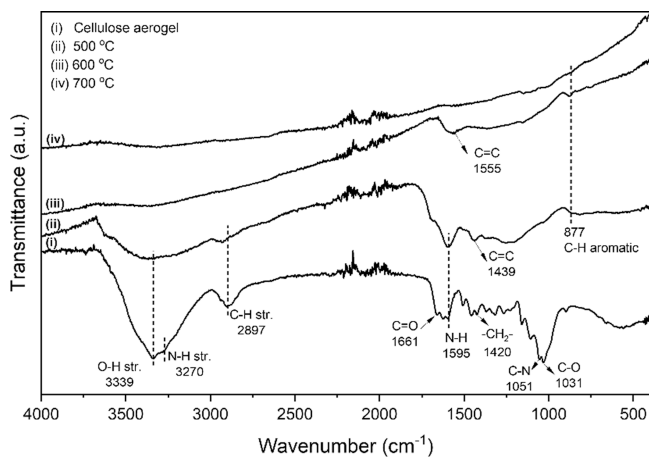


Figure 3. FTIR spectra of the cellulose aerogel (i) and its corresponding carbon aerogel obtained at various pyrolysis temperatures: (ii) 500 °C, (iii) 600 °C, and (iv) 700 °C.

amide C=O and C–N groups of urea, indicating the important role of urea as a cross-linking agent in the formation of cellulose aerogels. The presence of C–H stretching and –CH₂– vibration at wavenumbers of 2897 and 1420 cm⁻¹ indicated the existence of CH and CH₂ bonds in the cellulose structure.^{25,32} The C–O functional group was detected at the peak of 1031 cm⁻¹, which corresponds to the cellulose C–O–H group.³² FTIR spectra of the carbon aerogel obtained at a

temperature of 500 and 600 °C show an obvious band of C=C at 1439 cm⁻¹ and slightly shifts to 1555 cm⁻¹ due to polycyclic aromatic carbon ring formation. The band at 877 cm⁻¹ can be assigned to C–H aromatic.^{14,32} Pyrolysis at high temperatures leads to dehydration, which promotes the hydroxyl groups of cellulose to disengage and followed by dissociation of the C–O–C bond, resulting in the formation of aromatic polycyclic carbon rings.^{33,34} The bands disappeared at 700 °C because the hydroxyl groups had been evaporated completely. Cellulose also decomposed into volatile substances at this temperature and their phase changed into liquid and gas with a lower molecular weight.²⁸ The highest surface area of the carbon aerogel was obtained at a pyrolysis temperature of 700 °C, and this sample was treated further for sulfonation and hydrophobic modification. The results are discussed below.

3.2. Characteristics of the Hydrophobic SCA. Figure 4 presents the FTIR spectra of sulfonated and hydrophobically modified SCAs prepared using various mass ratios of the TBA-to-solid catalyst. Three typical bands are apparent in the spectra of SCAs at 1641, 1544, and 1409 cm⁻¹, which correspond to C=C functional groups.^{16,33,35} In addition to aromatic polycyclic carbon bonding originated from the carbon aerogel, the bands may come from the aromatic groups of benzene in sulfanilic acid grafted on the surface of carbon aerogels. Two bands at 1017 and 644 cm⁻¹ can be attributed to, respectively, the –SO₂– symmetric group and C–S group, confirming the successfulness of sulfonate grafting on the carbon surface.^{16,36} The band at 1544 cm⁻¹ that can be attributed to the C=C group is still apparent in the spectrum of all hydrophobically modified sulfonated carbons.^{16,36} For sulfonated carbon modified with a TBA-to-solid ratio of 0.3, a new band appears at 1148 cm⁻¹ that corresponds to asymmetric –SO₂– vibration from sulfonate groups grafted on the carbon surface. The intensity that characterizes sulfonate groups at 1104 cm⁻¹ weakens, which may be caused by hydrophobic agents that cover the groups.³⁷ These signals

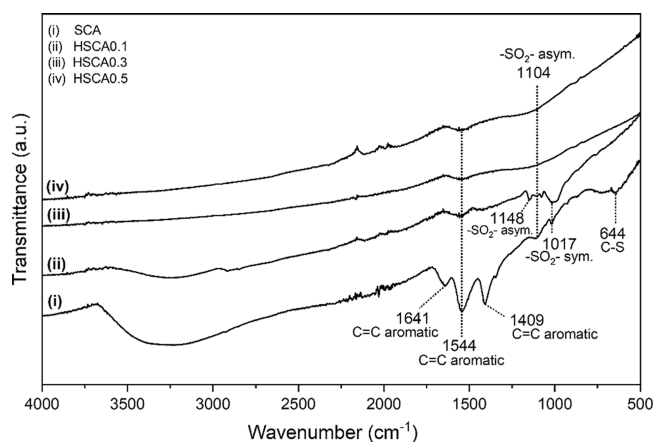


Figure 4. FTIR spectra of the SCA: (i) SCA, (ii) hydrophobic SCA with a mass ratio of TBA to SCA of 0.1:1 (HSCA0.1), (iii) mass ratio of TBA to SCA of 0.3:1 (HSCA0.3), and (iv) mass ratio of TBA to SCA of 0.5:1 (HSCA0.5).

indicate the successfulness of grafting the sulfonating and hydrophobic agents to the surface of the carbon aerogel.

Table 2 shows the properties of the hydrophobically modified SCA derived from coir fibers via the cellulose aerogel

Table 2. Properties of the Functionalized Carbon Aerogel

sample	TBA/ SCA ^a (g/ g)	acid density (mmol/g)	surface area (m ² g ⁻¹)	water contact angle (°)
SCA	0	2.81	3808.00	
HSCA0.1	0.1	2.70	3658.59	70
HSCA0.3	0.3	2.56	3586.37	94
HSCA0.5	0.5	2.30	3397.58	115

^aTBA/SCA: mass ratio of 4-*tert*-butylaniline/sulfonated carbon aerogel.

route. The acid densities determined by the titration method of all the prepared catalysts were in the range of 2.30 to 2.81 mmol g⁻¹. The acid density decreased when the catalyst was hydrophobically modified with TBA. During the modification process, TBA may be grafted on the surfaces of the sulfonated catalysts via covalent bonds, which likely caused the sulfonate groups to be covered and restricted from interacting with alkaline solution during titration.^{19,23} This also influenced the specific surface area of carbon aerogels, which decreased significantly after being modified with TBA. The decrease is larger with the increase of the TBA-to-solid ratio.^{19,23}

The changes in the surface hydrophilic–hydrophobic properties of the SCA before and after surface modification with TBA were examined by dispersing the aerogels into water and by measuring the water contact angle. For the unmodified SCA, the solid particles were immediately dispersed into the water body once they were dropped on the water surface. This is different for the case of the modified SCAs. As shown in Figure 5a, the solid particles floated on the water surface once they were dropped and then slowly some of the particles settled down into water due to gravity. Fewer particles settled down for the SCA modified with a higher TBA-to-solid ratio. These indicate that SCAs modified with a higher TBA-to-solid ratio are more hydrophobic. To be more quantitative, the contact angle of the water droplet dropped on the SCA surface was measured. Figure 5b shows that the shape of the water

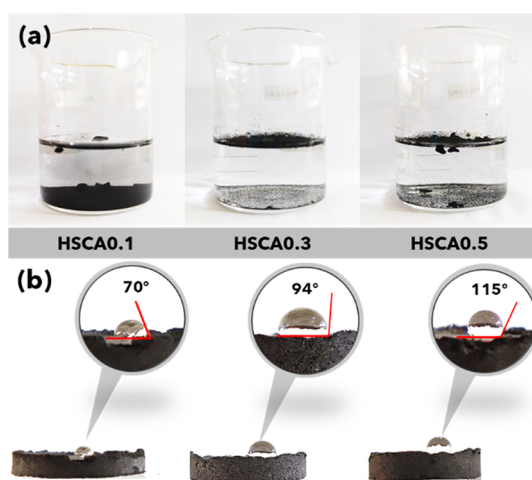


Figure 5. (a) Dispersion of the prepared hydrophobic SCA into water, and (b) water contact angles of the hydrophobic SCA.

droplet is more spherical for the SCA modified with a higher TBA-to-solid ratio, leading to a higher contact angle. The water contact angle increased with an increase in the amount of TBA grafted on the surface of the SCA. The highest water contact angle of 115° could be obtained using a TBA-to-solid ratio of 0.5, which corroborates the results obtained by the dispersing method.

The surface hydrophobicity properties of the SCA originate from sulfonic acid (SO₃H) moieties introduced on the carbon surface. After sulfonation, the carbon surface is partially covered by SO₃H moieties that show good affinity toward water molecules.³⁸ The SCA immersed immediately when dropped on the water surface and water dropped on the aerogel surface absorbed immediately and did not have a chance to form droplets. After TBA grafting, SCAs did not immerse immediately into water but stayed floating on the water surface for a sufficiently long time before some particles settled due to gravity. In addition, water could form droplets on the aerogel surface. During surface modification, parts of the SO₃H–carbon surface are capped by alkyl moieties that reduce the acid density as previously discussed. The alkyl moieties induce less affinity toward water molecules resulting in hydrophobic nature and water repellent properties.³⁹

3.3. Catalytic Esterification Reaction on the Catalyst.

To clarify the effect of surface hydrophobic modification of the SCA on the catalytic performance, esterification of acetic acid with ethanol was performed as a model reaction. Figure 6 presents the acetic acid conversion during esterification using the unmodified and hydrophobic modified catalysts at various reaction times. Although the acid density and the specific surface area of modified hydrophobic catalysts are lower, their conversion is higher than that obtained using the unmodified hydrophilic catalyst. For the unmodified hydrophilic catalyst, the conversion increased slowly with time and reached only about 27.93% at a reaction time of 180 min. On the other hand, the conversion increased rapidly when using modified hydrophobic catalysts and reached >66% for the first 30 min of reaction. At the end of the reaction (180 min), the conversion for all hydrophobic catalysts reached >70%. However, the catalytic performance seems less effective when the catalyst is strongly hydrophobic as shown by the decrease in conversion of the reaction catalyst with a water contact angle of 115°. Strong hydrophobicity of the catalyst surface has adverse effect

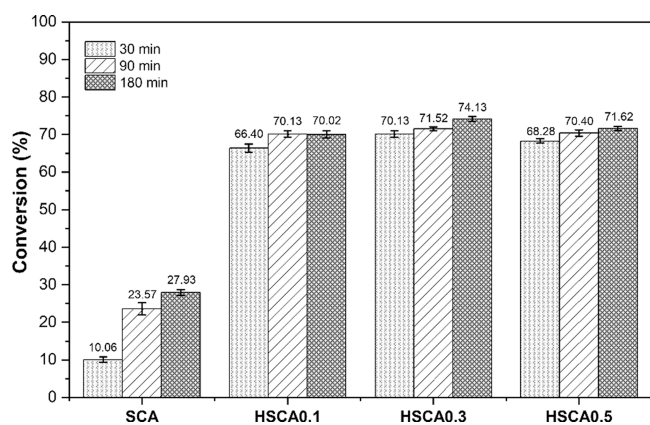


Figure 6. Conversion of acetic acid during the esterification reaction using the SCA catalysts at various reaction times.

on its catalytic performance for compounds containing oxygen and nonpolar moieties due to their strong attraction to the hydrophobic surface of the catalyst.^{23,40,41} In our case, esterification was performed using both reactants and the main product of organic compounds, which make desorption of products from the catalyst surface with high hydrophobicity more difficult due to the strong affinity between the catalyst and the product.

The results suggest that the acid side density and surface area are not the only parameters influencing the catalyst performance. As previously mentioned, the acid density and the specific surface area of the catalyst decreases with the amount of TBA added. Thus, the active side, specific surface area, and hydrophobicity of the catalyst significantly affect the activity of heterogeneous acid catalysts. For the esterification case that produce water as a byproduct, the hydrophobicity directly influences the conversion due to water repelled from the surface that induces a forward reaction. On the contrary, hydrophilic surfaces lead to the adsorption of water on the catalyst surface. This adsorption has a potential to block the catalyst pores and the active sides. Moreover, the hydrophobic surface of the catalyst can promote the adsorption of organic reactants in the catalytic reaction system and restrict the reverse reaction.^{14,19,23,42}

4. CONCLUSIONS

In summary, the hydrophobic solid acid catalyst was successfully prepared by pyrolysis of cellulose aerogels derived from coir fibers using sulfanilic acid as the sulfonating agent and TBA as the hydrophobic agent. The highest specific surface area of 3911.047 m² g⁻¹ was achieved at 700 °C, and this sample was subsequently processed further for sulfonation and hydrophobization. The hydrophobicity of the catalyst surface could be adjusted by introducing TBA via the diazo reduction method to the sulfonated carbon. Meanwhile, both acid density and surface area of the carbon aerogel decreased when a higher amount of TBA was added. This study reveals that acid density and specific surface area are not the only parameters affecting the catalyst performance. The surface hydrophobicity of the solid acid catalyst also plays an important role in the catalytic performance of catalysts for reactions producing water as a byproduct such as esterification reactions.

AUTHOR INFORMATION

Corresponding Author

Heru Setyawan – Department of Chemical Engineering, Faculty of Industrial Technology and System Engineering, Sepuluh Nopember Institute of Technology, Surabaya 60111, Indonesia; orcid.org/0000-0002-2158-6819; Phone: +62 31 5946240; Email: sheru@chem-eng.its.ac.id; Fax: +62 31 5999282

Authors

Ade Sonya Suryandari – Department of Chemical Engineering, Faculty of Industrial Technology and System Engineering, Sepuluh Nopember Institute of Technology, Surabaya 60111, Indonesia; Department of Chemical Engineering, Politeknik Negeri Malang, Malang 65141, Indonesia; Present Address: On leave from Politeknik Negeri Malang (A.S.S. permanent affiliation)

Tantular Nurtono – Department of Chemical Engineering, Faculty of Industrial Technology and System Engineering, Sepuluh Nopember Institute of Technology, Surabaya 60111, Indonesia

Widiyastuti Widiyastuti – Department of Chemical Engineering, Faculty of Industrial Technology and System Engineering, Sepuluh Nopember Institute of Technology, Surabaya 60111, Indonesia; orcid.org/0000-0002-2805-2836

Complete contact information is available at:

<https://pubs.acs.org/10.1021/acsomega.3c02244>

Notes

The authors declare no competing financial interest.

ACKNOWLEDGMENTS

This research was supported by Institut Teknologi Sepuluh Nopember through a Scientific Research Grant (Contract No. 953/PKS/ITS/2022). One of the authors (A.S.S.) thank Higher Education Financing Center (Balai Pembiayaan Pendidikan Tinggi - BPPT) and Indonesia Endowment Funds for Education (Lembaga Pengelola Dana Pendidikan - LPDP) for providing a doctoral scholarship through the BPI Program. We thank Ms. Mega Putri Nurmalasari, Ms. Iffat Rizki Qatrunada, and Mr. Sudibyo Enggar Laksono for their assistance with the experiments.

REFERENCES

- Macario, A.; Giordano, G.; Onida, B.; Cocina, D.; Tagarelli, A.; Giuffrè, A. M. Biodiesel Production Process by Homogeneous/Heterogeneous Catalytic System Using an Acid-Base Catalyst. *Appl. Catal., A* **2010**, *378*, 160–168.
- Tariq, M.; Ali, S.; Khalid, N. Activity of Homogeneous and Heterogeneous Catalysts, Spectroscopic and Chromatographic Characterization of Biodiesel: A Review. *Renewable Sustainable Energy Rev.* **2012**, *16*, 6303–6316.
- Bashir, M. A.; Wu, S.; Zhu, J.; Krosuri, A.; Khan, M. U.; Ndeddy Aka, R. J. Recent Development of Advanced Processing Technologies for Biodiesel Production: A Critical Review. *Fuel Process. Technol.* **2022**, *227*, No. 107120.
- Borges, M. E.; Díaz, L. Recent Developments on Heterogeneous Catalysts for Biodiesel Production by Oil Esterification and Transesterification Reactions: A Review. *Renewable Sustainable Energy Rev.* **2012**, *16*, 2839–2849.
- Syazwani, O. N.; Rashid, U.; Mastuli, M. S.; Taufiq-Yap, Y. H. Esterification of Palm Fatty Acid Distillate (PFAD) to Biodiesel Using

- Bi-Functional Catalyst Synthesized from Waste Angel Wing Shell (Cyrtoptera Costata). *Renewable Energy* **2019**, *131*, 187–196.
- (6) Boey, P. L.; Ganesan, S.; Maniam, G. P.; Khairuddean, M.; Efendi, J. A New Heterogeneous Acid Catalyst for Esterification: Optimization Using Response Surface Methodology. *Energy Convers. Manage.* **2013**, *65*, 392–396.
- (7) Hykkerud, A.; Marchetti, J. M. Esterification of Oleic Acid with Ethanol in the Presence of Amberlyst 15. *Biomass Bioenergy* **2016**, *95*, 340–343.
- (8) Mulyatun, M.; Prameswari, J.; Istadi, I.; Widayat, W. Production of Non-Food Feedstock Based Biodiesel Using Acid-Base Bifunctional Heterogeneous Catalysts: A Review. *Fuel* **2022**, *314*, No. 122749.
- (9) Zhou, Y.; Niu, S.; Li, J. Activity of the Carbon-Based Heterogeneous Acid Catalyst Derived from Bamboo in Esterification of Oleic Acid with Ethanol. *Energy Convers. Manage.* **2016**, *114*, 188–196.
- (10) Kiss, F. E.; Jovanović, M.; Bošković, G. C. Economic and Ecological Aspects of Biodiesel Production over Homogeneous and Heterogeneous Catalysts. *Fuel Process. Technol.* **2010**, *91*, 1316–1320.
- (11) Wang, X.; Liu, R.; Waje, M. M.; Chen, Z.; Yan, Y.; Bozhilov, K. N.; Feng, P. Sulfonated Ordered Mesoporous Carbon as a Stable and Highly Active Protonic Acid Catalyst. *Chem. Mater.* **2007**, *19*, 2395–2397.
- (12) Liu, R.; Wang, X.; Zhao, X.; Feng, P. Sulfonated Ordered Mesoporous Carbon for Catalytic Preparation of Biodiesel. *Carbon* **2008**, *46*, 1664–1669.
- (13) Xing, R.; Liu, Y.; Wang, Y.; Chen, L.; Wu, H.; Jiang, Y.; He, M.; Wu, P. Active Solid Acid Catalysts Prepared by Sulfonation of Carbonization-Controlled Mesoporous Carbon Materials. *Micro-porous Mesoporous Mater.* **2007**, *105*, 41–48.
- (14) Fauziyah, M.; Widiyastuti, W.; Setyawan, H. Sulfonated Carbon Aerogel Derived from Coir Fiber as High Performance Solid Acid Catalyst for Esterification. *Adv. Powder Technol.* **2020**, *31*, 1412–1419.
- (15) Yu, H.; Jin, Y.; Li, Z.; Peng, F.; Wang, H. Synthesis and Characterization of Sulfonated Single-Walled Carbon Nanotubes and Their Performance as Solid Acid Catalyst. *J. Solid State Chem.* **2008**, *181*, 432–438.
- (16) Mardhiah, H. H.; Ong, H. C.; Masjuki, H. H.; Lim, S.; Pang, Y. L. Investigation of Carbon-Based Solid Acid Catalyst from *Jatropha Curcas* Biomass in Biodiesel Production. *Energy Convers. Manage.* **2017**, *144*, 10–17.
- (17) Tohdee, K.; Semmad, S.; Jotisankasa, A.; Praserttham, P.; Jongsomjit, B. Investigation of Sulfonated Solid Acid Catalysts Derived from Oil Palm Kernel Shell, Corn cob, and Diatomaceous Earth for Esterification of Ethanol and Propanoic Acid, Characterisation and Their Performance. *Bioresour. Technol. Rep.* **2021**, *16*, No. 100855.
- (18) Zhong, R.; Sels, B. F. Sulfonated Mesoporous Carbon and Silica-Carbon Nanocomposites for Biomass Conversion. *Appl. Catal., B* **2018**, *236*, 518–545.
- (19) Zhong, Y.; Deng, Q.; Zhang, P.; Wang, J.; Wang, R.; Zeng, Z.; Deng, S. Sulfonic Acid Functionalized Hydrophobic Mesoporous Biochar: Design, Preparation and Acid-Catalytic Properties. *Fuel* **2019**, *240*, 270–277.
- (20) Wallach, R. Physical Characteristics of Soilless Media. In *Soilless Culture: Theory and Practice*; Raviv, M. R., Lieth, J. H., Eds.; Elsevier: Boston, 2008; pp 41–116.
- (21) Sari, R. M.; Gea, S.; Wirjosentono, B.; Hendrana, S.; Torres, F. G. The Effectiveness of Coconut Coir as Tar Adsorbent in Liquid Smoke Integrated into the Pyrolysis Reactor. *Case Stud. Therm. Eng.* **2021**, *25*, No. 100907.
- (22) Fauziyah, M.; Widiyastuti, W.; Setyawan, H. Nitrogen-Doped Carbon Aerogels Prepared by Direct Pyrolysis of Cellulose Aerogels Derived from Coir Fibers Using an Ammonia-Urea System and Their Electrocatalytic Performance toward the Oxygen Reduction Reaction. *Ind. Eng. Chem. Res.* **2020**, *59*, 21371–21382.
- (23) Zhong, Y.; Zhang, P.; Zhu, X.; Li, H.; Deng, Q.; Wang, J.; Zeng, Z.; Zou, J. J.; Deng, S. Highly Efficient Alkylation Using Hydrophobic Sulfonic Acid-Functionalized Biochar as a Catalyst for Synthesis of High-Density Biofuels. *ACS Sustainable Chem. Eng.* **2019**, *7*, 14973–14981.
- (24) Niu, S.; Ning, Y.; Lu, C.; Han, K.; Yu, H.; Zhou, Y. Esterification of Oleic Acid to Produce Biodiesel Catalyzed by Sulfonated Activated Carbon from Bamboo. *Energy Convers. Manage.* **2018**, *163*, 59–65.
- (25) Setyawan, H.; Fauziyah, M.; Tomo, H. S. S.; Widiyastuti, W.; Nurtono, T. Fabrication of Hydrophobic Cellulose Aerogels from Renewable Biomass Coir Fibers for Oil Spillage Clean-Up. *J. Polym. Environ.* **2022**, *30*, 5228–5238.
- (26) Zuo, L.; Zhang, Y.; Zhang, L.; Miao, Y. E.; Fan, W.; Liu, T. Polymer/Carbon-Based Hybrid Aerogels: Preparation, Properties and Applications. *Materials* **2015**, *8*, 6806–6848.
- (27) Long, L. Y.; Weng, Y. X.; Wang, Y. Z. Cellulose Aerogels: Synthesis, Applications, and Prospects. *Polymers* **2018**, *10*, 623.
- (28) Thangalazhy-Gopakumar, S.; Adhikari, S.; Ravindran, H.; Gupta, R. B.; Fasina, O.; Tu, M.; Fernando, S. D. Physicochemical Properties of Bio-Oil Produced at Various Temperatures from Pine Wood Using an Auger Reactor. *Bioresour. Technol.* **2010**, *101*, 8389–8395.
- (29) Novak, J. M.; Busscher, W. J.; Laird, D. L.; Ahmedna, M.; Watts, D. W.; Niandou, M. A. S. Impact of Biochar Amendment on Fertility of a Southeastern Coastal Plain Soil. *Soil Sci.* **2009**, *174*, 105–112.
- (30) Yang, C.; Liu, J.; Lu, S. Pyrolysis Temperature Affects Pore Characteristics of Rice Straw and Canola Stalk Biochars and Biochar-Amended Soils. *Geoderma* **2021**, *397*, No. 115097.
- (31) Lu, S.; Zong, Y. Pore Structure and Environmental Serves of Biochars Derived from Different Feedstocks and Pyrolysis Conditions. *Environ. Sci. Pollut. Res.* **2018**, *25*, 30401–30409.
- (32) Pavia, D. L.; Lampman, G. M.; Kriz, G. S.; Vyvyan, J. R. *Introduction to Spectroscopy*, 4th ed.; Lockwood, L., Kirksey, B., Woods, E., Eds.; Brooks/Cole: California, 2009.
- (33) Cheng, F.; Li, X. Preparation and Application of Biochar-Based Catalysts for Biofuel Production. *Catalysts* **2018**, *8*, 346.
- (34) Liu, W. J.; Jiang, H.; Yu, H. Q. Development of Biochar-Based Functional Materials: Toward a Sustainable Platform Carbon Material. *Chem. Rev.* **2015**, *115*, 12251–12285.
- (35) Tang, X.; Niu, S. Preparation of Carbon-Based Solid Acid with Large Surface Area to Catalyze Esterification for Biodiesel Production. *J. Ind. Eng. Chem.* **2019**, *69*, 187–195.
- (36) Ibrahim, N. A.; Rashid, U.; Taufiq-Yap, Y. H.; Yaw, T. C. S.; Ismail, I. Synthesis of Carbonaceous Solid Acid Magnetic Catalyst from Empty Fruit Bunch for Esterification of Palm Fatty Acid Distillate (PFAD). *Energy Convers. Manage.* **2019**, *195*, 480–491.
- (37) Sandouqa, A.; Al-Hamamre, Z.; Asfar, J. Preparation and Performance Investigation of a Lignin-Based Solid Acid Catalyst Manufactured from Olive Cake for Biodiesel Production. *Renewable Energy* **2019**, *132*, 667–682.
- (38) Kamegawa, T.; Mizuno, A.; Yamashita, H. Hydrophobic Modification of SO₃H-Functionalized Mesoporous Silica and Investigations on the Enhanced Catalytic Performance. *Catal. Today* **2015**, *243*, 153–157.
- (39) Nazriati, N.; Setyawan, H.; Affandi, S.; Yuwana, M.; Winardi, S. Using Bagasse Ash as a Silica Source When Preparing Silica Aerogels via Ambient Pressure Drying. *J. Non-Cryst. Solids* **2014**, *400*, 6–11.
- (40) Cavuoto, D.; Zaccheria, F.; Ravasio, N. Some Critical Insights into the Synthesis and Applications of Hydrophobic Solid Catalysts. *Catalysts* **2020**, *10*, 1337.
- (41) Zhong, Y.; Deng, Q.; Yao, Q.; Lu, C.; Zhang, P.; Li, H.; Wang, J.; Zeng, Z.; Zou, J. J.; Deng, S. Functionalized Biochar with Superacidity and Hydrophobicity as a Highly Efficient Catalyst in the Synthesis of Renewable High-Density Fuels. *ACS Sustainable Chem. Eng.* **2020**, *8*, 7785–7794.
- (42) Wolska, J.; Stawicka, K.; Walkowiak-Kulikowska, J. Sulfonic-Acid-Functionalized Polymers Based on Fluorinated Methylstyrenes and Styrene as Promising Heterogeneous Catalysts for Esterification. *Mater. Chem. Phys.* **2021**, *273*, No. 125132.